Defence Research and Development Canada
Recherche et développement pour la défense Canada

DEFENCE R&D DÉFENSE

Two-dimensional adaptive processing for ionospheric clutter mitigation in high frequency surface wave radar

R.J. Riddolls

Defence R&D Canada – Ottawa
Technical Memorandum
DRDC Ottawa TM 2008-319
December 2008

Canada

Two-dimensional adaptive processing for ionospheric clutter mitigation in high frequency surface wave radar

R. J. Riddolls
Defence R&D Canada – Ottawa

Defence R&D Canada – Ottawa
Technical Memorandum
DRDC Ottawa TM 2008-319
December 2008

Principal Author

Original signed by R. J. Riddolls

R. J. Riddolls

Approved by

Original signed by D. Dyck

D. Dyck
Head/Radar Systems Section

Approved for release by

Original signed by P. Lavoie

P. Lavoie
Head/Document Review Panel

Abstract

High Frequency Surface Wave Radar (HFSWR) is a technology used for over-the-horizon detection of ocean vessels. This radar exploits the diffraction of electromagnetic waves around the curved surface of the earth. To minimize the attenuation of the diffracted waves, the radar must operate at frequencies in the lower part of the high frequency (HF) band. However, radar signals at these frequencies also reflect from the earth's ionosphere, which leads to radar clutter at ranges beyond 200 km. The linear broadside receive arrays used by conventional HFSWR cannot filter out this clutter as the arrays do not have any resolving power in elevation angle. Reported here are theoretical and experimental investigations of the clutter suppression capability of one- and two-dimensional HFSWR adaptive processors. Three configurations are compared: one-dimensional spatial adaptive processing, two-dimensional spatial adaptive processing, and space-time adaptive processing. In all cases the number of adaptive degrees of freedom is 16. It is found that the best results are achieved by two-dimensional spatial adaptive processing, where a processing gain of up to about 20 dB can be achieved.

Résumé

Le radar haute fréquence à ondes de surface (HFSWR) est une technologie utilisée pour détecter des navires situés au-delà de l'horizon. Le radar exploite la diffraction des ondes électromagnétiques situées autour de la surface courbée de la terre. Pour minimiser l'affaiblissement des ondes diffractées, le radar doit exploiter les fréquences de la partie inférieure de la bande haute fréquence (HF). Toutefois, à ces fréquences, les signaux radars sont réfléchis par l'ionosphère, ce qui produit du clutter radar au-delà de 200 km. Les antennes réseau à réception transversale qu'utilise habituellement le HFSWR sont incapables de filtrer ce clutter, car elles n'ont pas de pouvoir de résolution dans l'angle de site. Le présent document fait état des enquêtes théoriques et expérimentales sur la capacité qu'ont les processeurs adaptatifs HFSWR unidimensionnels et bidimensionnels de supprimer le clutter. Les trois configurations à comparer sont : le traitement adaptatif spatial unidimensionnel ; le traitement adaptatif spatial bidimensionnel ; le traitement adaptatif espace/temps. Dans tous les cas, on compte 16 degrés de liberté adaptatifs. On juge que le traitement adaptatif spatial bidimensionnel produit les meilleurs résultats, soit un gain d'antenne de 20 dB.

This page intentionally left blank.

Executive summary

Two-dimensional adaptive processing for ionospheric clutter mitigation in high frequency surface wave radar

R. J. Riddolls; DRDC Ottawa TM 2008-319; Defence R&D Canada – Ottawa; December 2008.

High Frequency Surface Wave Radar (HFSWR) can detect ocean vessels beyond the horizon by employing the propagation of the Norton surface wave over the conducting ocean surface. To minimize surface wave attenuation, HFSWR usually operates in the 2–6 MHz band, permitting detection of targets out to the boundary of the 200-nautical mile Exclusive Economic Zone (EEZ). Frequencies in this band also reflect from the ionosphere, leading to radar clutter beyond 200 km in range. Unfortunately, the linear broadside receive arrays used by conventional HFSWR have no resolving power in elevation angle to filter clutter. Thus, alternative two-dimensional adaptive processing schemes are studied with the aim to maximize clutter suppression.

Performance assessment requires knowledge of the space-time correlation of signals reflected from the ionosphere. We adopt a first-principles physical model using analytic ray tracing in a plane-stratified ionosphere containing small-scale density irregularities. An expression is derived for the space-time correlation function of the signal complex amplitude, and this function is used to compute the predicted space-time covariance matrix of signals observed by the radar receiving array. The covariance matrix is in turn used to predict the signal-to-noise ratio improvement afforded by a particular adaptive array configuration, referred to as the array gain. Calculations are made for a one-dimensional spatial adaptive processor, a two-dimensional spatial adaptive processor, and a space-time adaptive processor.

The two-dimensional adaptive processor consists of a beamformer that combines the signals received by the elements of a 4×4 square planar array. Both theoretical and experimental results show that array performance depends on the array steer direction with respect to the earth's magnetic field. The two-dimensional adaptive array provides an experimentally verified array gain of 19 dB when steered north-south and 9 dB when steered east-west. The one-dimensional spatial adaptive processor and space-time adaptive processor utilize linear arrays and provide experimentally verified gains of 11 dB and 14 dB, respectively, when the target is along the axis of the array. The gains decay to 4 dB and 5 dB, respectively, when the target moves to a position broadside to the array. For comparison purposes, complete clutter cancellation in the data sets studied would require an array gain of about 35 dB. Thus the two-dimensional receive array can be viewed as a partial solution, and should be considered in concert with other clutter cancellation techniques, such as adaptive

transmit-side beamforming.

Sommaire

Two-dimensional adaptive processing for ionospheric clutter mitigation in high frequency surface wave radar

R. J. Riddolls; DRDC Ottawa TM 2008-319; R & D pour la défense Canada – Ottawa; décembre 2008.

Le radar haute fréquence à ondes de surface (HFSWR) peut détecter des navires situés au-delà de l'horizon grâce à la propagation d'ondes de surface Norton sur la surface conductrice de l'océan. Pour minimiser l'affaiblissement des ondes de surface, le HFSWR fonctionne habituellement dans la bande 2-6 MHz. Cela lui permet de détecter des cibles situées au delà des limites de la zone d'exclusion économique (ZEE) de 200 milles marins. Les fréquences de cette bande sont également réfléchies par l'ionosphère, ce qui engendre du clutter radar au delà de 200 km. Malheureusement, les antennes réseau linéaires à réception transversale qu'utilisent les HFSWR traditionnels n'ont pas de pouvoir de résolution dans l'angle de site pour filtrer ce clutter. Donc, dans le but de supprimer le plus possible le clutter, des schémas de traitement adaptatif bidimensionnels sont étudiés.

L'évaluation du rendement requiert la connaissance de la corrélation spacio temporelle des signaux réfléchis par l'ionosphère. Nous adoptons un modèle physique de base fondé sur le tracé analytique de rayons dans une ionosphère stratifiée en plan qui contient des irrégularités de densité à petite échelle. Une expression est dérivée pour la fonction de corrélation spacio-temporelle de l'amplitude complexe du signal et on utilise cette fonction pour calculer la matrice de covariance spacio temporelle des signaux captés par le réseau récepteur du radar. La matrice de corrélation sert ensuite à prévoir l'amélioration du rapport signal/bruit qu'assure une configuration de l'antenne adaptative, que l'on appelle gain d'antenne. On effectue des calculs pour un processeur adaptatif spatial unidimensionnel, un processeur adaptatif spatial bidimensionnel, et un processeur adaptatif espace/temps.

Le processeur adaptatif bidimensionnel consiste en un conformateur de faisceau qui combine les signaux par les éléments d'un réseau plan carré 4 x 4. Les résultats théoriques et expérimentaux démontrent que le rendement du réseau dépend de son orientation par rapport au champ magnétique terrestre. Le réseau adaptatif bidimensionnel produit un gain d'antenne vérifié expérimentalement de 19 dB lorsqu'il est orienté du nord au sud, et de 9 dB lorsqu'il est orienté d'est en ouest. Le processeur adaptatif spatial unidimensionnel et le processeur adaptatif espace/temps utilisent des réseaux linéaires et, lorsque la cible est située sur l'axe du réseau, ces processeurs produisent des gains d'antenne vérifiés expérimentalement de 11 dB et de 14 dB respectivement. Lorsque les cibles se trouvent en position trasnversale par rapport au

réseau, les gains sont réduits à 4 dB et à 5 dB respectivement. Pour fins de comparaisons, l'annulation totale du clutter pour les séries de données étudiées nécessiterait un gain d'antenne d'environ 35 dB. On peut donc considérer le réseau de réception bidimensionnel comme une solution partielle qui devrait être prise en considération au même titre que les autres techniques d'annulation de clutter, comme la conformation adaptative de faisceau du côté émetteur.

Table of contents

List of figures

1 Introduction

High Frequency Surface Wave Radar (HFSWR) is a technology that permits detection of ocean vessels beyond the horizon by exploiting the propagation of the Norton surface wave. To minimize surface wave attenuation, long-range HFSWR usually operates in the 2–6 MHz band, permitting detection of targets out to the boundary of the 200-nautical mile Exclusive Economic Zone (EEZ). Frequencies in this band also reflect from the earth's ionosphere, leading to radar clutter beyond 200 km in range. Unfortunately, the linear broadside receive arrays used by conventional HFSWR have no resolving power in elevation angle to remove clutter. Thus, a planar array is studied with the intent to use its elevation-filtering capabilities to mitigate ionospheric clutter [1].

Array performance assessment requires knowledge of the space-time correlation of signals reflected from the ionosphere. We adopt a first-principles physical model that uses analytic ray tracing in a plane-stratified ionosphere containing small-scale density irregularities. The model has appeared in several versions in the literature [2, 3, 4], and the incarnation used here was developed by the author previously to study other aspects of HF radar performance [5]. It differs from previous versions in that it assumes a plane-stratified ionosphere and allows for a fully anisotropic plasma refractive index and anisotropic spectrum for the density perturbations.

The lowest-order effect is a scintillation of the signal phase. An expression is derived in Chapter 2 for the two-point space-time correlation function of the signal complex amplitude, and in Chapter 3 this function is used to compute the predicted space-time covariance matrix of signals observed by the radar receiver, which is in turn used to predict the signal-to-noise ratio improvement afforded by various adaptive processors, referred to as the array gain. Calculations are made for a 16-element linear array, referred to as one-dimensional spatial adaptive processing (1-D SAP), a 4×4 square planar array, referred to as two-dimensional spatial adaptive processing (2-D SAP), and finally a space-time adaptive processor (STAP) consisting of 4 linear elements, each with 4 time samples. In Chapter 4, the performance of these processors is illustrated by analysing data from two recent experiments.

2 Derivation of signal correlation

This section describes the form of the signal spatial correlation function based on an analytic ray tracing theory. Ray tracing in an irregular medium has been used for a number of propagation studies [2, 3, 4], and the form presented here summarizes [5], which describes propagation in a plane-stratified anisotropic ionosphere (also see [6, 7]). The theory details the perturbation of a radar pulse in location, group delay, frequency, and wavenumber. Here we will concern ourselves with the frequency and wavenumber perturbation, as these perturbations will be used to determine the performance of adaptive processors in Chapter 3.

The spectrum of the phase of the ionospheric clutter signal is given by [5]

$$S_\phi(\kappa_x, \kappa_y, \Omega) = \int dz \left(\frac{\partial k_z}{\partial N}\right)^2 S_{N_1}(\kappa_x, \kappa_y, \kappa_z = 0, \Omega). \tag{1}$$

Here, N is the plasma density, N_1 is the density irregularity, z is vertical upward, x is east, y is north, and k_z is the vertical radar wavenumber at altitude z. For S_{N_1} we use a spectrum model for plasma irregularities that follows a spatial 4th-order power law and a dispersion relation for near-perpendicular drift waves [8]:

$$S_{N_1}(\boldsymbol{\kappa}, \Omega) = \frac{4\sqrt{2\alpha}\pi^2 E[N_1^2(z)]\kappa_0^{-3}}{1 + \kappa_0^{-4}(\kappa_\perp^2 + \alpha\kappa_\parallel^2)^2}\delta(|\Omega| - \kappa_\perp v_d). \tag{2}$$

Here, v_d is the diamagnetic drift velocity (≤ 60 m/s), κ_0 is the outer scale length ($\approx 10^{-4}$ m^{-1}), α is an anisotropy factor, $\kappa_\perp$ is the magnitude of the component of the density irregularity wavenumber $\boldsymbol{\kappa}$ that is perpendicular to the earth's magnetic field, $\kappa_\parallel$ is the magnitude of the component of $\boldsymbol{\kappa}$ along the field, and the variance of the density fluctuations $E[N_1^2(z)]$ is assumed to be a function of altitude z. We suppose the magnetic field of the earth follows a unit vector $\hat{\mathbf{l}} = (l_x, l_y, l_z)$. Quantities $\kappa_\parallel$ and $\kappa_\perp$ are:

$$\kappa_\parallel = \boldsymbol{\kappa} \cdot \hat{\mathbf{l}} \qquad \kappa_\perp = ||\boldsymbol{\kappa} - \kappa_\parallel \hat{\mathbf{l}}||. \tag{3}$$

Although z is constrained to be vertical, at this point we can rotate x and y azimuthally without loss of generality such that the magnetic field vector lies in the y-z plane and $l_x = 0$. Therefore we conclude that

$$S_\phi(\kappa_x, \kappa_y, \Omega) = \frac{4\sqrt{2\alpha}\pi^2\kappa_0^{-3}\delta[|\Omega| - (\kappa_x^2 + l_z^2\kappa_y^2)^{1/2}v_d]}{1 + \kappa_0^{-4}[\kappa_x^2 + (l_z^2 + \alpha l_y^2)\kappa_y^2]^2} \int dz\, E[N_1^2(z)] \left(\frac{\partial k_z}{\partial N}\right)^2. \tag{4}$$

On the basis of $\alpha \gg 1$, we assume that the spectrum is negligible when $\kappa_x \approx \kappa_y$. This allows the form of the delta function and the denominator to be simplified. For now, we also ignore the scalar amplitude of the spectrum for simplicity. Thus,

$$S_\phi(\kappa_x, \kappa_y, \Omega) \propto \frac{\delta(|\Omega| - |\kappa_x| v_d)}{1 + \kappa_0^{-4}(\kappa_x^2 + \alpha l_y^2 \kappa_y^2)^2}. \tag{5}$$

The space-time autocorrelation of the phase is given by the inverse Fourier transform:

$$R_\phi(X,Y,T) \propto \iiint d\kappa_x d\kappa_y d\Omega \; S_\phi \, e^{i\kappa_x X + i\kappa_y Y - i\Omega T}$$
$$\propto \iint d\kappa_x d\kappa_y \frac{e^{i\kappa_x X + i\kappa_y Y'}(e^{i\kappa_x v_d T} + e^{-i\kappa_x v_d T})}{1 + \kappa_0^{-4}(\kappa_x^2 + \kappa_y^2)^2}. \quad (6)$$

where $Y' = Y/(\sqrt{\alpha} l_y)$. The integration is most easily carried out in polar co-ordinates as follows [9]:

$$R_\phi(X,Y,T) \propto \sum_{m=1,-1} \int_0^\infty \int_0^{2\pi} du \, d\psi \, \frac{u e^{iu\kappa_0 \sqrt{(X+mv_dT)^2 + Y'^2}\cos\psi}}{1+u^4}$$
$$\propto \sum_{m=1,-1} \int_0^\infty du \, \frac{u J_0(u\kappa_0 \sqrt{(X+mv_dT)^2 + Y'^2})}{1+u^4}$$
$$\propto \sum_{m=1,-1} \int_{-\infty}^\infty du \, \frac{u H_0^{(1)}(u\kappa_0 \sqrt{(X+mv_dT)^2 + Y'^2})}{1+u^4}, \quad (7)$$

To evaluate the integral, we form a closed contour in the upper half plane enclosing the poles at $e^{i\pi/4}$ and $e^{3i\pi/4}$. Using the residue theorem [10], it can be shown that

$$R_\phi(X,Y,T) \propto \sum_{m=1,-1} \mathrm{kei}(\kappa_0 \sqrt{(X+mv_dT)^2 + Y'^2}), \quad (8)$$

where kei is a Kelvin function, defined as [11]

$$\mathrm{ker}(x) + i\mathrm{kei}(x) = \frac{\pi i}{2} H_0^{(1)}(x e^{3\pi i/4}). \quad (9)$$

The autocorrelation at zero lag is simply the mean-square phase fluctuation $E(\phi^2)$. Since $\mathrm{kei}(0) = -\pi/4$, we can write

$$R_\phi(X,Y,T) = -\frac{2}{\pi} E(\phi^2) \sum_{m=1,-1} \mathrm{kei}(\kappa_0 \sqrt{(X+mv_dT)^2 + Y'^2}). \quad (10)$$

The central limit theorem implies Gaussian single-point statistics for ϕ. Thus, we can relate R_ϕ to the autocorrelation of the complex signal amplitude $A = e^{i\phi}$ using [12]:

$$E\left[e^{-i\phi(x,y,t)} e^{i\phi(x+X,y+Y,t+T)}\right] = e^{R_\phi(X,Y,T) - E(\phi^2)}. \quad (11)$$

Thus, the required complex amplitude autocorrelation function is

$$R_A(X,Y,T) = \exp\left\{ -E(\phi^2) \left[1 + \frac{2}{\pi} \sum_{m=1,-1} \mathrm{kei}(\kappa_0 \sqrt{(X+mv_dT)^2 + Y'^2}) \right] \right\}, \quad (12)$$

from which array performance can be determined.

3 Adaptive processor gain

We consider a surface vessel radar echo consisting of a plane wave of amplitude a that is received by an array of antenna elements arranged in an arbitrary configuration. In the case of SAP, the amplitude and phase response of the individual sensors to the plane wave target signal is captured by an array manifold vector $\mathbf{v}$. In the case of STAP, the response to the plane wave target signal across sensors and pulses is captured by a space-time steering vector, which will also be denoted by $\mathbf{v}$. Both cases can be treated within the same framework.

In addition to the plane wave signal, the sensors are corrupted by a "noise" vector $\mathbf{n}$ that is dominated by ionospheric clutter signals. Thus the signal measured by the array can be written as

$$\mathbf{b} = \mathbf{v}a + \mathbf{n}. \tag{13}$$

We devise a linear estimator for a that consists of summing the measured signals according to a "weight" function $\mathbf{w}$. This estimator is denoted as $\hat{a} = \mathbf{w}^H\mathbf{b}$, where H is the complex conjugate transpose. In order to minimize the variance of the expected value $E(\hat{a})$ under the constraint of no distortion $E(\hat{a}) = E(a)$, the optimal choice of weights for this linear estimator is given by [13]:

$$\mathbf{w}^H = \frac{\mathbf{v}^H\mathbf{R}_n^{-1}}{\mathbf{v}^H\mathbf{R}_n^{-1}\mathbf{v}}, \tag{14}$$

where $\mathbf{R}_n = E(\mathbf{n}\mathbf{n}^H)$ is the noise covariance matrix. This processor is distortionless, so it provides no improvement in target signal power. All SNR improvement arises from reducing noise power associated with the ionospheric clutter. At the input to the adaptive processor, the noise power associated with each spatial element or temporal pulse is given by the diagonal entries of $\mathbf{R}_n$. To help quantify the reduction in this noise power by the processor, we assume the data is calibrated such that the noise power is constant across all elements and times, and equal to a scalar denoted by R_n. The noise power at the output of the processor is thus given by

$$R_{\hat{a}} = \mathbf{w}^H\mathbf{R}_n\mathbf{w} = \frac{1}{\mathbf{v}^H\mathbf{R}_n^{-1}\mathbf{v}}. \tag{15}$$

The SNR gain of the processor, denoted as the array gain, is

$$G_A = R_n/R_{\hat{a}} = R_n\mathbf{v}^H\mathbf{R}_n^{-1}\mathbf{v} \equiv \mathbf{v}^H\mathcal{R}_n^{-1}\mathbf{v}. \tag{16}$$

Here, $\mathcal{R}_n$ is a normalized covariance matrix where the entries on the matrix diagonal are unity. In the case of uncorrelated noise, the array gain will be simply $G_A = \mathbf{v}^H\mathbf{v} = N$, where N is the number of sensors. In the case of correlated noise, the array gain could be more or less than N.

To compute the normalized array covariance matrix $\mathcal{R}_n$, we evaluate the spatial autocorrelation function R_A, given by Equation (12), at the spatial and temporal signal sampling locations (X, Y, T). This procedure has been carried out for three processor types: 1-D SAP, 2-D SAP, and STAP. In the 1-D SAP case, the samples are made by 16 sensors in a linear array. In the 2-D SAP case, there are also 16 sensors, but arranged in a 4×4 square planar array. Finally, in the STAP case, there are 4 sensors in a linear array and 4 temporal samples taken from each sensor. In each of the 1-D SAP and STAP cases, two orientations are considered: the linear array is either oriented magnetic north-south (i.e., in the magnetic meridian plane) or magnetic east-west. In the 2-D SAP case, only one orientation is considered such that the edges of the array are parallel with the magnetic north-south and east-west directions.

To compare the various processors, we calculate the variation of array gain with target azimuth angle. The reference angle will be magnetic north, such that zero degrees is broadside for the east-west linear array and endfire for the north-south linear array. The sensor spatial separation is 33.33 m, the temporal sampling period is 1.024 seconds, and the operating frequency is 3.2 MHz, which are chosen to approximate the experimental conditions described in the following chapter. For illustrative purposes, we assume a root mean-square phase scintillation $\sqrt{E(\phi^2)} = 200$ radians and an aspect ratio $\sqrt{\alpha} = 3$.

The results are shown in Figure 1. Five curves are displayed. The solid curves correspond to the north-south and east-west array orientations for 1-D SAP. In the north-south case, the target angle transitions from endfire to broadside as target angle increases. The array gain is maximum at endfire and minimum at broadside. The reason for this behavior is easy to understand. Since the linear array is at ground level, vertically incident ionospheric clutter is always broadside to the array. Thus, when the target is endfire, the target and clutter have distinct sensor-to-sensor phase relationships that are easy to separate, leading to good array gain. However, when the target is broadside, both the target and clutter produce nearly constant phase across all the sensors. The target and clutter signals cannot be easily distinguished, resulting in poor array gain.

We now discuss the east-west array orientation of 1-D SAP. In Figure 1, the target angle transitions from broadside to endfire as target angle increases. The same general features are observed as in the north-south case: the broadside array gain is worse than the endfire gain. However, the difference is less pronounced than in the north-south case. The reason is that the spatial covariance function of the clutter is "stretched" in the north-south direction due to the aspect ratio of the irregularities. In precise terms, the $1/(\sqrt{\alpha} l_y)$ scale factor relating the X (east-west) and Y' (north-south) co-ordinates in Equation (12) means that the clutter is more strongly correlated from sensor to sensor in the north-south direction than in the east-west

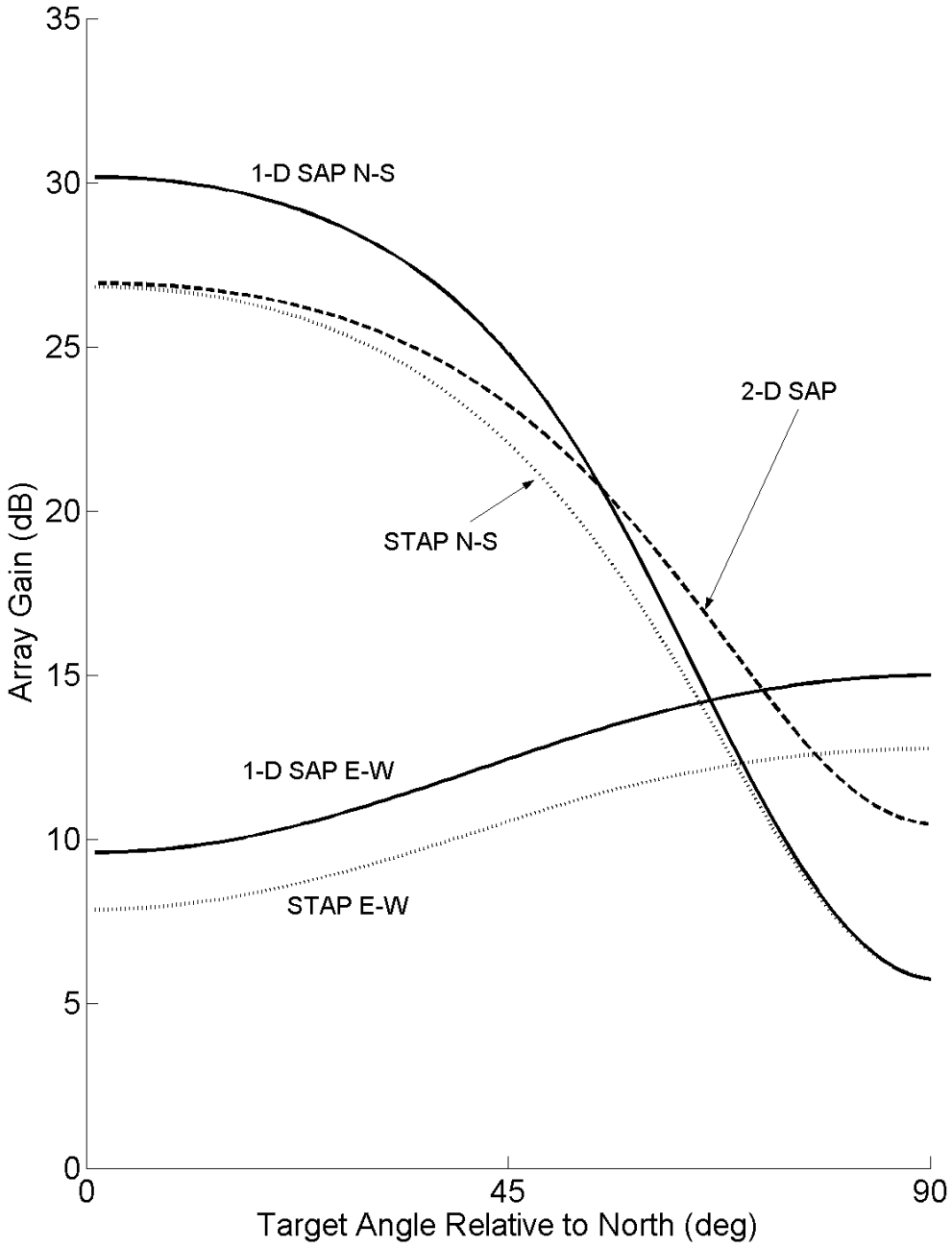

Figure 1: *Array gain versus target azimuth angle.*

direction. This permits greater adaptive array gain when the array is oriented north-south. One can think of the aspect ratio as skewing the curves in Figure 1 so that the array gains are raised on the left side of the plot.

The 2-D SAP processor represents a compromise between the east-west and north-south orientations of 1-D SAP. It is shown as a dashed line in Figure 1. The planar array sensor-to-sensor phase relationships will always be different for clutter and target. The ionospheric clutter signal phase fronts simultaneously arrive at all sensors, whereas the target signal arrives at successive rows of sensors in the array with large row-to-row phase lags. This permits good adaptive array gain at all angles. The slant in the curve in Figure 1 arises entirely because of the assumed aspect ratio of the irregularities.

The STAP case, shown as dotted lines in Figure 1, is particularly interesting. Inspection of the correlation function, Equation (12), suggests that the time axis is similar to a second spatial axis, and therefore the STAP covariance matrix should have similar structure to the sensor covariance matrix of a 2-D SAP planar array. However, the plotted curves of array gain show that STAP is closely related to 1-D SAP. The reason lies in the target steering vector. The spatial part of the STAP processor is much like 1-D SAP. The temporal part of STAP exploits the phase relationship between successive time samples (or "pulses"). Low-speed targets produce low Doppler shifts relative to the radar waveform repetition frequency, which implies small pulse-to-pulse phase variation in the target signal. These targets thus behave as broadside targets in the temporal part of the STAP processor, regardless of the target azimuth angle. Therefore the STAP performance versus target angle is dominated by the spatial component of the processor, and so the STAP array gain curves follow somewhat the behavior of the 1-D SAP curves. One can achieve better array gain by using more adaptive degrees of freedom in the STAP processor, but one runs into difficulty in finding a sufficient number of radar range gate samples from which to estimate the clutter covariance. More advanced techniques aimed at mitigating this problem will not be addressed here.

4 Experiments

To illustrate the processing schemes outlined in the previous chapter, data from two experiments were analysed. In the first experiment, the DRDC Transportable High Frequency Surface Wave Radar was fielded at the DRDC Ottawa campus to collect echoes from the ionosphere using a two-dimensional 4×4 array of receive elements. This experiment allows 2-D SAP performance assessment for a 16-element planar array. In the second experiment, data were analyzed from a Canadian Navy HFSWR at Cape Race, Newfoundland, which features a linear array of 16 receive elements, and permits testing of 1-D SAP and STAP schemes.

4.1 Planar receive array experiment description

In April 2005, an experiment was conceived by the author to demonstrate the effectiveness of a planar array in mitigating HFSWR ionospheric clutter. A site was selected at the DRDC Ottawa campus to deploy the radar. The reason for locating the radar in Ottawa was to minimize logistical complications. However, the Ottawa location has the disadvantage that there is no nearby ocean. The collected data has only ionospheric echoes and no ocean echoes or mixed-path ionosphere-ocean echoes. An array was installed at the site in late 2005. In March 2006, the DRDC Transportable HFSWR was brought out to the site and the array was connected to the radar. Hardware malfunctions delayed acquisition of data until September 2007.

The experiment apparatus features a two-dimensional receive array of 16 vertical monopole elements arranged in a 4×4 square with an inter-element spacing of 33.33 m, as shown in Figure 2. The axes of the square are aligned with the magnetic north-south and magnetic east-west directions in order to facilitate comparisons with theory. The center of the receive array is located at N45°21'33" W75°53'05". The transmit antenna consists of a triangular loop antenna oriented in a vertical plane aligned magnetic north-south, as shown in Figure 3. The antenna is 10 meters tall

Figure 2: *Two-dimensional receive array.*

Figure 3: *Transmit antenna.*

and 40 meters wide, and is tuned such that at the antenna terminals, the impedance is pure real 200 ohms at the assigned radar operating frequency of 3.281 MHz. This antenna is connected to the radar transmitter through a 4:1 impedance tranformation balun. A power level of 1 kW peak envelope power is used in the experiments, which is constrained by the power handling capacity of the antenna and balun. The waveform is an 8-bit Frank Code [14]. The range resolution is about 10 km, the pulse repetition rate is 125 Hz, and the waveform repetition rate is 15.625 Hz. The data is collected by 16 receivers sampling at a rate of 100 kilosamples per second, which corresponds to 1.5-km range gates. The data is pulse-compressed and stored in a range-time-channel format. A total of 270 range gates spanning the range 62.0 km to 465.5 km are retained by the radar, and data sets are partitioned into a coherent integration time (CIT) lasting 512 waveform repetitions (32.768 s).

Results presented here were acquired on 24 Septemper 2007 between 0300 and 0400 UTC (11 pm to midnight the previous day in Eastern Daylight Saving Time). It was necessary to operate the radar pre-midnight local time since the ionosphere tended to decay to a peak critical frequency less than 3.281 MHz after midnight.

4.2 Linear receive array experiment

The second experiment reported here was carried out using an experimental HFSWR at Cape Race, Newfoundland in March 2002. This same radar was later acquired by the Canadian Navy in 2003.

In the Cape Race radar configuration, ocean vessels are illuminated by a single “flood-

light" log-periodic array of vertical monopoles, and the ship echoes are acquired by a 16-element broadside linear array of "doublet" elements. Each doublet consists of a forward and rear pair of vertical monopoles that are combined with fixed phasing to maximize gain in the forward direction and minimize gain in the reverse direction. Each doublet comprises a radar data channel acquired by the radar receiver. The boresight of the entire array is oriented 143 degrees clockwise from magnetic north. Effects of different array orientations with respect to magnetic north were not investigated.

Results to be presented were acquired on 25 Mar 2002 between 0230 and 0330 UTC (11 pm to midnight the previous day in Newfoundland Standard Time). The radar was operated at a frequency of 3.1 MHz. The radar timing parameters are the same as in the planar array experiment.

4.3 Experiment results

Results from the experiments are shown in Figure 4. All of the panels show ionospheric clutter as a large broad structure located in the region >350 km. Cells around the clutter are occupied by external noise. For illustration, a synthetic target has been inserted into the data at 300 km range and zero Doppler. The target is spread over several range cells to simulate the limited range resolution of the radar waveform.

The top row of the figure compares single-channel data (left panel) with 1-D SAP when the target is located at broadside (middle panel) and endfire (right panel). The broadside case shows an insignificant reduction (about 4 dB) in clutter level. This is consistent with the predictions of Chapter 2, which suggest that the adaptive processing gain is a minimum for broadside orientation. In contrast, the endfire case shows a more noticeable reduction in the clutter (about 11 dB), which is also consistent with the prediction that cancellation maximizes at endfire.

The middle row of the figure shows the comparison of single-channel data (left panel) with 2-D SAP for an eastward target (middle panel) and 2-D SAP for a northward target (right panel). For the eastward target, the suppression is about 9 dB and for the northward target, the suppression is about 19 dB. Once again, this is consistent with the idea presented in Figure 1 that the aspect ratio of the irregularities tends to increase clutter correlation in the north-south direction, allowing for better cancellation in that direction. It is interesting to note that the background atmospheric noise in the area surrounding the clutter does not have the same property, and as a result, is equally cancelled by both processors.

The bottom row shows the effect of STAP processing. We have chosen a set of 4 contiguous spatial channels from the linear array and 4 temporal pulses that are separated by 1.024 seconds. The covariance matrix is estimated using range samples.

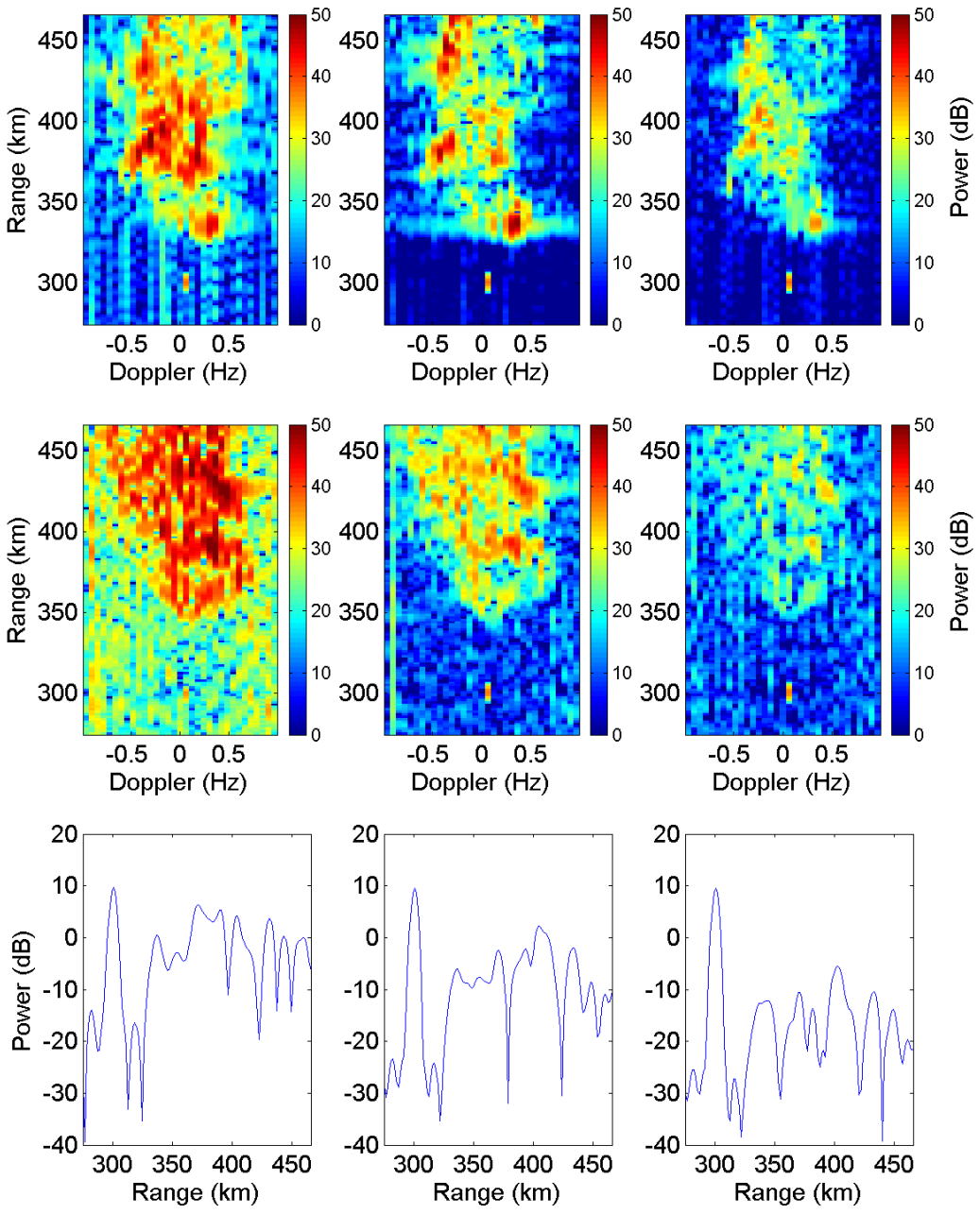

Figure 4: *Top row, left to right: single channel, 1-D SAP broadside, 1-D SAP endfire. Middle row, left to right: single channel, 2-D SAP aimed east, 2-D SAP aimed north. Bottom row, left to right: single channel, STAP broadside, STAP endfire.*

The data shows a comparison of single-channel data (left panel) versus STAP for a broadside array (middle panel), and an endfire array (right panel). The broadside cancellation is about 5 dB and the endfire cancellation is about 14 dB. This behaviour is similar to the 1-D SAP results, as was predicted by the theory.

These examples suggest that the 2-D array shows the best performance, although performance comparisons are not rigorous since the data in the two experiments were taken at different times and the level of RMS phase scintillation could vary (nevertheless, the Doppler spread of the signals suggests at least a similar scintillation level). Furthermore, the level of clutter statistical inhomogeneity has not been characterized, so local homogeneity has to be assumed. For example, in the SAP cases, the pulses are used for training the adaptive filter, so it is assumed that the spatial statistics do not vary over the period of the coherent integration time (32.768 s). If faster adaptation is required, one would need to choose adaptive weights that vary within the CIT [15].

5 Conclusion

This memorandum has briefly reported on the matter of two-dimensional adaptive processing for reducing ionospheric clutter in High Frequency Surface Wave Radar (HFSWR) data. This clutter is an issue for radar operations since the conventional HFSWR linear broadside receive arrays have no resolving power in elevation angle.

In order to assess performance of the proposed schemes, the space-time correlation function of signals reflected from the ionosphere was derived in Chapter 2. This formulation used a first-principles physical model consisting of analytic ray tracing in a plane-stratified ionosphere containing small-scale density irregularities.

In Chapter 3 the space-time correlation function was used to compute the predicted space-time covariance matrix of signals observed by the radar receiver, which in turn was used to predict the array gain afforded by a particular array configuration. Calculations were made for one- and two-dimensional spatial adaptive processing (1-D and 2-D SAP) as well as space-time adaptive processing (STAP). In all cases, 16 adaptive degrees of freedom were used. 2-D SAP provided an experimentally verified gain of about 19 dB for northward targets and about 9 dB for eastward targets. 1-D SAP and STAP processors were not effective at broadside, but provided average gains of about 11 dB and 14 dB, respectively, for target signals at endfire. However, one should keep in mind that the use of linear arrays at endfire leads to poor azimuth resolving capability since the endfire resolving power scales with the squareroot of the number of elements instead of directly with the number of elements as in the broadside case.

Finally, it should be noted that the 20-dB processing gain associated with the 2-D SAP was not sufficient to push the clutter to the noise floor—an additional improvement of approximately 15 dB is required. This additional gain could be achieved by either more degrees of freedom in the adaptive processor or by employing adaptive transmit beamformers. Adaptive transmit beamformers will be discussed in a future paper.

References

[1] Abramovich, Y., Anderson, S., Lyudviga, Y., Spencer, N., Turcaj, P., and Hibble, B. (2004). Space-time adaptive techniques for ionospheric clutter mitigation in HF surface wave radar systems, In *Proceedings of the 2004 International Conference on Radar Systems*, Toulouse, France.

[2] Basler, R. P., Price, G. H., Tsunoda, R. T., and Wong, T. L. (1988). Ionospheric distortion of HF signals. *Radio Science*, 23 (4), 569–579.

[3] Roth, M., Muller, G., and Snieder, R. (1993). Velocity shift in random media. *Geophysics Journal International*, 115, 552–563.

[4] Coleman, C. J. (1996). A model of HF sky wave radar clutter. *Radio Science*, 31 (4), 869–875.

[5] Riddolls, R. J. (2006). A model of radio wave propagation in ionospheric irregularities for prediction of high-frequency radar performance. (DRDC Ottawa TM2006-284). Defence R&D Canada – Ottawa.

[6] Budden, K. G. (1985). The propagation of radio waves: the theory of radio waves of low power in the ionosphere and magnetosphere. Cambridge, UK: Cambridge University Press.

[7] Booker, H. G. (1936). Oblique propagation of electromagnetic waves in a slowly-varying non-isotropic medium. *Proceedings of the Royal Society of London*, A. 155, 411–451.

[8] Rufenach, C. L. (1975). Ionospheric scintillation by a random phase screen: spectral approach. *Radio Science*, 10 (2), 155–165.

[9] Walsh, J. (2006). Private communication.

[10] Saff, E. B. and Snider, A. D. (1993). Fundamentals of complex analysis for mathematics, science, and engineering, 2nd ed. Englewood Cliffs, New Jersey: Prentice Hall, p. 250.

[11] Abramowitz, M. and Stegun, I. A. (1964). Handbook of mathematical functions, Applied Mathematics Series 55, National Bureau of Standards, p. 379.

[12] Reed, I. S. (1962). On a moment theorem for complex Gaussian processes. *IRE Transactions on Information Theory*, 8 (4), 194–195.

[13] Capon, J. (1969). High-resolution frequency-wavenumber spectrum analysis. *Proceedings of the IEEE*, 57 (8), 1408–1418.

[14] Chan, H. C. (2003). Characterization of ionospheric clutter in HF surface-wave radar. (DRDC Ottawa TR 2003-114). Defence R&D Canada – Ottawa.

[15] Fabrizio, G. A., Gershman, A. B., and Turley, M. D. (2004). Robust adaptive beamforming for HF surface wave over-the-horizon radar. *IEEE Transactions on Aerospace and Electronic Systems*, 40 (2), 510-525.

This page intentionally left blank.

DOCUMENT CONTROL DATA

(Security classification of title, body of abstract and indexing annotation must be entered when the overall document is classified)

1. ORIGINATOR (the name and address of the organization preparing the document. Organizations for whom the document was prepared, e.g. Establishment sponsoring a contractor's report, or tasking agency, are entered in section 8.)

Defence R&D Canada - Ottawa
Ottawa, Ontario, K1A 0Z4

2. SECURITY CLASSIFICATION (overall security classification of the document, including special warning terms if applicable)

UNCLASSIFIED

3. TITLE (the complete document title as indicated on the title page. Its classification should be indicated by the appropriate abbreviation (S,C or U) in parentheses after the title.)

Two-dimensional adaptive processing for ionospheric clutter mitigation in high frequency surface wave radar

4. AUTHORS (Last name, first name, middle initial)

Riddolls, Ryan J.

5. DATE OF PUBLICATION (month and year of publication of document)

December 2008

6a. NO. OF PAGES (total containing information. Include Annexes, Appendices, etc.)

28

6b. NO. OF REFS (total cited in document)

15

7. DESCRIPTIVE NOTES (the category of the document, e.g. technical report, technical note or memorandum. If appropriate, enter the type of report, e.g. interim, progress, summary, annual or final. Give the inclusive dates when a specific reporting period is covered.)

Technical Memorandum

8. SPONSORING ACTIVITY (the name of the department project office or laboratory sponsoring the research and development. Include the address.)

Defence R&D Canada - Ottawa
Ottawa, Ontario, K1A 0Z4

9a. PROJECT OR GRANT NO. (if appropriate, the applicable research and development project or grant number under which the document was written. Please specify whether project or grant)

Project 11hh

9b. CONTRACT NO. (if appropriate, the applicable number under which the document was written)

10a. ORIGINATOR'S DOCUMENT NUMBER (the official document number by which the document is identified by the originating activity. This number must be unique to this document.)

DRDC Ottawa TM 2008-319

10b. OTHER DOCUMENT NOS. (Any other numbers which may be assigned this document either by the originator or by the sponsor)

11. DOCUMENT AVAILABILITY (any limitations on further dissemination of the document, other than those imposed by security classification)

(x) Unlimited distribution
( ) Distribution limited to defence departments and defence contractors; further distribution only as approved
( ) Distribution limited to defence departments and Canadian defence contractors; further distribution only as approved
( ) Distribution limited to government departments and agencies; further distribution only as approved
( ) Distribution limited to defence departments; further distribution only as approved
( ) Other (please specify):

12. DOCUMENT ANNOUNCEMENT (any limitation to the bibliographic announcement of this document. This will normally correspond to the Document Availability (11). However, where further distribution (beyond the audience specified in 11) is possible, a wider announcement audience may be selected.)

Unlimited

13. ABSTRACT (a brief and factual summary of the document. It may also appear elsewhere in the body of the document itself. It is highly desirable that the abstract of classified documents be unclassified. Each paragraph of the abstract shall begin with an indication of the security classification of the information in the paragraph (unless the document itself is unclassified) represented as (S), (C), or (U). It is not necessary to include here abstracts in both official languages unless the text is bilingual).

High Frequency Surface Wave Radar (HFSWR) is a technology used for over-the-horizon detection of ocean vessels. This radar exploits the diffraction of electromagnetic waves around the curved surface of the earth. To minimize the attenuation of the diffracted waves, the radar must operate at frequencies in the lower part of the high frequency (HF) band. However, radar signals at these frequencies also reflect from the earth's ionosphere, which leads to radar clutter at ranges beyond 200 km. The linear broadside receive arrays used by conventional HFSWR cannot filter out this clutter as the arrays do not have any resolving power in elevation angle. Reported here are theoretical and experimental investigations of the clutter suppression capability of one- and two-dimensional HFSWR adaptive processors. Three configurations are compared: one-dimensional spatial adaptive processing, two-dimensional spatial adaptive processing, and space-time adaptive processing. In all cases the number of adaptive degrees of freedom is 16. It is found that the best results are achieved by two-dimensional spatial adaptive processing, where a processing gain of up to about 20 dB can be achieved.

14. KEYWORDS, DESCRIPTORS or IDENTIFIERS (technically meaningful terms or short phrases that characterize a document and could be helpful in cataloguing the document. They should be selected so that no security classification is required. Identifiers such as equipment model designation, trade name, military project code name, geographic location may also be included. If possible keywords should be selected from a published thesaurus. e.g. Thesaurus of Engineering and Scientific Terms (TEST) and that thesaurus-identified. If it is not possible to select indexing terms which are Unclassified, the classification of each should be indicated as with the title.)

HIGH FREQUENCY
RADAR
OVER THE HORIZON
SKY WAVE
SURFACE WAVE
RADIO
PROPAGATION
IONOSPHERE
PLASMA
IRREGULARITIES
CLUTTER
ANTENNA
ARRAY

Defence R&D Canada

Canada's leader in Defence
and National Security
Science and Technology

R & D pour la défense Canada

Chef de file au Canada en matière
de science et de technologie pour
la défense et la sécurité nationale

www.drdc-rddc.gc.ca